STM JOURNALS

Journal of
Polymer & Composites

ISSN: 2321-2810 (Online)
ISSN: 2321-8525 (Print)
Volume 11, Special Issue 13, 2023
DOI (Journal): 10.37591/JoPC

http://engineeringjournals.stmjournals.in/index.php/JoPC/index

Research JoPC

Revolutionizing Geopolymer Composites: Unveiling Intelligent Wall Facades and Precision PZT Sensors for Vibration Analysis

Moulya H.V.[1,*], Chandrashekar A.[2], Ananthayya M.B.[3]

Abstract

Evaluating the mechanical performance and environmental benefits of geopolymer composites is imperative for sustainable alternatives in construction. This study presents an innovative circular PZT-based sensor that effectively captures transient vibrations within concrete structures, demonstrating its validity in comparison to standard surface-mounted accelerometers. The research also elucidates the influence of sensor orientation on capturing various vibrational modes of concrete. Furthermore, the embedded PZT sensors provide valuable insights into the evolving mechanical properties of hydrating concrete, offering a continuous measure of concrete stiffness as it ages. In the context of geopolymer concrete, the study showcases its environmental benefits by comparing it with conventional cement-based concrete in the form of interlocking paver blocks. The results reveal that geopolymer concrete, particularly the variant incorporating 100% GGBS, exhibits superior compressive strength, reaching 92.17 N/mm² compared to 54.2 N/mm² for conventional concrete. Additionally, PZT sensors successfully identify cracks in geopolymer composite, highlighting its potential for improved mechanical properties and reduced environmental impact in the construction industry.

Keywords: Geopolymer composites, PZT Sensor, Interlock, Fly ash, and GGBS

INTRODUCTION

Concrete, renowned for its unparalleled versatility and exceptional durability, has stood as the cornerstone of modern construction for generations [1]. Nevertheless, the conventional production of concrete reliant on Portland cement raises formidable environmental concerns owing to the substantial carbon emissions intrinsic to cement manufacturing. In response to this pressing challenge, both researchers and industry professionals have embarked on a quest to explore alternative construction materials and methodologies that reconcile sustainability with uncompromised performance. One such pioneering material at the forefront of this movement is geopolymer concrete, heralded as a greener and more efficient substitute for traditional concrete. Geopolymer concrete is ingeniously crafted by inducing reactions between aluminosilicate source materials and alkaline activators, rendering the use of Portland cement obsolete [2]. This environmentally conscious approach not only significantly mitigates carbon emissions but also harnesses industrial by-products like fly ash and ground granulated blast furnace slag (GGBS), thereby diverting them away from landfills.

***Author for Correspondence**
Moulya H.V.

[1]Assistant Professor, Department of Civil Engineering, Nitte Meenakshi Institute of Technology, Visvesvaraya Technological University, Bengaluru, Karnataka, India
[2]Professor & Head, Department of Civil Engineering, KVG College of Engineering, Visvesvaraya Technological University, Dakshina Kannada, Karnataka, India
[3] Professor & Head, department of Civil Engineering, Sai Vidya Institute of Technology, Visvesvaraya Technological University, Bengaluru, Karnataka, India

Received Date: November 17, 2023
Accepted Date: December 14, 2023
Published Date: March 06, 2024

Citation: Moulya H.V., Chandrashekar A., Ananthayya M.B. Revolutionizing Geopolymer Composites: Unveiling Intelligent Wall Facades and Precision PZT Sensors for Vibration Analysis. Journal of Polymer & Composites. 2023; 11(Special Issue 13): S59–S73.

Consequently, geopolymer concrete is rapidly gaining recognition and consideration for an array of construction applications, ranging from wall facing elements to interlocking paver blocks and beyond [3]. However, as with any emerging material, the adoption of geopolymer concrete in the realm of construction necessitates rigorous scrutiny and continuous monitoring to guarantee its structural integrity and long-term performance. Among the critical aspects of this evaluation, the detection and assessment of vibrations emerge as paramount, offering invaluable insights into the mechanical behavior and overall integrity of concrete structures. These vibrations can emanate from diverse sources, including environmental factors, equipment operations, or structural movements [4].

Traditionally, the evaluation of vibrations and mechanical properties of concrete structures has leaned on conventional methods such as surface-mounted accelerometers and visual inspections. While these approaches have proven effective to a certain extent, they often prove labor-intensive, time-consuming, and may fail to deliver continuous, real-time evaluations of concrete performance. Moreover, they may fall short in identifying subtle, low-level, transient vibrations that transpire during the crucial initial stages of concrete setting and curing [5]. To surmount these limitations and elevate the monitoring and assessment of geopolymer concrete wall facing elements and other concrete structures to a more sophisticated level, a smart sensing approach encompassing embedded sensors becomes indispensable. This approach not only facilitates real-time vibration detection but also harbors the potential to capture invaluable data concerning the evolving mechanical properties of the concrete. In this context, the integration of lead zirconate titanate (PZT) sensors, celebrated for their sensitivity to transient dynamic motion, assumes relevance [6]. The following sections of this paper delve into the profound significance of geopolymer concrete in the context of wall facing elements and underscore the critical imperative for a smart sensing approach that leverages PZT sensors to propel the monitoring and evaluation of concrete structures into the future. This paper further explores the capabilities of embedded PZT sensors in the detection of vibrations and assessment of concrete properties, illuminating their potential to revolutionize construction industry practices while bolstering environmental sustainability [7].

Notably, the environmental concerns associated with conventional concrete production, particularly the high carbon emissions linked to OPC, underscore the urgency of transitioning to more eco-friendly alternatives. OPC manufacturing alone contributes significantly to global greenhouse gas emissions, accounting for approximately 7% of total emissions worldwide. Moreover, cement production stands as one of the most energy-intensive industrial processes, devouring about 4 gigajoules per ton. In India, the cement industry, trailing only thermal power plants and steel production, constitutes a substantial consumer of coal [8, 9]. Despite the robust demand for cement, projected to grow at a staggering 10% annually in India, the industry's environmental footprint remains a critical concern. In response to these challenges, innovative applications have emerged, utilizing both Fly Ash (FA) and Ground Granulated Blast Furnace Slag (GGBS) in the construction sector through Geopolymer Concrete (GPC) [10]. This pioneering approach leverages advanced processing techniques to harness various classes and grades of FA and GGBS, presenting a compelling opportunity to significantly reduce the stockpiles of these waste materials. Geopolymer concrete, characterized as inorganic polymer composites, represents a promising avenue for sustainable construction practices. GPC boasts attributes such as high strength and resistance against chloride penetration and acid attacks. Typically, GPC is formulated through alkali activation of industrial alumino-silicate waste materials, including FA and GGBS. Crucially, GPC offers a substantially reduced environmental footprint compared to conventional concrete options, a fact underscored by prior research findings [11]. Within the realm of construction, wall facing elements, such as panels, play an indispensable role, necessitating a comprehensive understanding of their mechanical properties and behavior. Recent research endeavors [12] underscore the significance of characterizing the properties of geopolymer-based wall facing elements to guarantee their structural integrity and enduring performance. Equally vital in ensuring resilient and crack-free wall facing elements are modern techniques such as MATLAB-based crack detection. These techniques offer

efficient means for identifying and quantifying cracks, thereby contributing to enhanced quality control and maintenance strategies. In light of these considerations, this study sets out [13] to explore the mechanical characteristics of FA-GGBS-based geopolymer concrete wall facing elements and subsequently employs MATLAB [14] for effective crack detection. Through these investigations, this research seeks to advance the comprehension and application of sustainable construction materials, shedding light on the promising future that geopolymer concrete offers within the construction industry.

LITERATURE SURVEY

In the [15] employed an energy-diffusing approach using active piezoelectric sensing to locate cracks. Signals emitted by actuators and captured by sensors were analyzed with the detection range influenced by the angles of specimen cuts and the distances between actuators and sensors. The study emphasized the preference for energy diffusivity, specifically focusing on ultrasound's energy propagation, using frequencies ranging from 50 kHz to 100 kHz. The detectable range analysis involved one actuator, three sensors, and four cut grooves, demonstrating effective crack detection within a ±15º circular sector for the sensing system. In 2018, a study [16] focused on the development of rubberized geopolymer interlocking bricks by incorporating crumb rubber instead of fine aggregate. The research involved conducting tests for compressive strength, flexural strength, water absorption, and efflorescence. The study found that higher sodium hydroxide (NaOH) molarity contributed to increased compressive strength, along with higher alkaline solution-fly ash ratios. The optimal compressive strength of 4.21 MPa was attained with a ratio of 0.8 and an 18 M NaOH concentration. The average flexural strength was 0.258 MPa, with optimal results obtained at a minimum ratio of 0.4 and a 10 M molarity.

A study explored concrete beam failure mechanisms, revealing that simple beams exhibited brittle failure through flexural cracks, whereas heavily reinforced beams lacking transverse reinforcement experienced shear failure characterized by diagonal cracks [17]. Key factors influencing ultimate failure and load-bearing capacity included aggregate meshing and steel bar dowel action. The research observed that shear stress transmission in prestressed concrete was not exclusively determined by deformation softening, and it noted that ultimate shear forces surpassed burst shear forces in the tested conditions. A study investigated Interlocking Block as Wall Panels using nominal bricks (210 x 105 x 75 mm) and interlocking blocks (280 × 125 × 100 mm) made of Class F fly ash [18]. Various tests, including compressive strength, water absorption, bond strength, impact, shear, efflorescence, soundness, and hardness, were conducted. The nominal brick exhibited a compressive strength of 7.62 N/mm², while interlocking blocks showed average strengths of 8.89 N/mm² at 14 days and 9.72 N/mm² at 28 days, indicating an up to 27.55% increase in interlock strength compared to nominal bricks. Furthermore, the impact resistance of interlocking blocks was 83.33% greater [19].

In a study focusing on cracks in synthetic fiber concrete beams, the investigation involved testing twelve beams (six unreinforced and six reinforced) for bending behavior, post-crack performance, and crack patterns [20]. The incorporation of a 1% synthetic fiber mix notably enhanced the behavior of unreinforced concrete after cracking, leading to a reduction in overall cracks. Additionally, beams with a 1% fiber content demonstrated a higher load-bearing capacity, such as 24.5 KN for 1.52 mm cracks, compared to 5.3 KN with a 0.5% fiber mix [21]. The study centered on the application of deep learning and structured light for the detection and measurement of concrete cracks. Using two laser sensors and structured light, the researchers identified cracks on concrete surfaces. The YOLO algorithm [22] facilitated real-time object detection, ensuring swift processing, while laser sensors, supported by a laser correction algorithm and distance sensors, accurately determined crack sizes. The inclusion of 1800 images of cracks and pseudo cracks into YOLOv3-tiny contributed to the enhancement of software accuracy. In testing with 150 images, the software achieved a commendable 94% accuracy and 98% precision, with a minimal crack size measurement error of less than 1.5 mm [23, 24]. When subjected to compressive loads, the structural characteristics of interlocking prisms

deviated from conventional masonry due to the distinctive contact mechanisms among components. Tests conducted on these interlocking prisms [25] revealed a pronounced stress concentration at the web shell, leading to a 53% reduction in compressive strength attributed to the slenderness ratio. To address this, strengthening methods such as filling holes with concrete grout or reinforcement bars were employed. The masonry treated with grout exhibited a significantly higher ultimate load, surpassing the ungrouted counterpart by 96.23%. Additionally, the incorporation of crumb rubber enhanced density, contributing to effective waste management [26-27]. Furthermore, the substitution of aggregate with fly ash resulted in a notable 10–20% increase in both compressive and flexural strength.

MATERIALS AND METHODS

The materials and procedures employed in this investigation are outlined, followed by a detailed explanation of the experimental configuration. The materials used in the study for making geopolymer and conventional concrete are:

Geopolymer Composites and Conventional Concrete

The geopolymer concrete MSand process integrates aluminosilicate components, specifically FA and GGBS, along with coarseaggregate, manufactured sand, alkali activator solutions and a super-plasticizer. In contrast, traditional concrete comprises 53-grade cement, Msand, coarseaggregate, and water. Tables 1, 2, 3, 4, and 5 provide a comprehensive overview of the chemical composition of aluminosilicate materials and the relevant physical properties of the concrete constituents employed in geopolymer concrete production.

Table 1. Chemical composition of cement.

Chemical Name	CaO	SiO_2	Al_2O_3	Fe_2O_3	MgO	SO_3	P_2O_5	K_2O	Na_2O	TiO_2
Chemical composition (%)	58.78	16.34	7.95	5.38	2.32	1.99	1.67	2.73	1.50	0.28

Table 2. Chemical composition of fly ash and GGBS.

Materials	Chemical Composition in Percentage							
	SiO_2	CaO	Al_2O_3	MgO	MnO	Fe_2O_3	SO_3	Chlorides
GGBS	35.27	31.25	21.20	8.46	0.05	1.65	079	0.03
Fly ash	55.57	2.84	32.97	0.92	0.02	5.51	0.46	0.04

Table 3. Physical properties of the concrete materials.

Description	Cement	Fly Ash	GGBS	Fine Aggregate (M Sand)	Coarse Aggregate
Specific Gravity	3.00	2.53	2.86	2.69	2.62
Specific Surface Area (m^2/kg)	340	333	370	-	-
Bulk Density (kg/m^3)	1865	1226	1280	1462	1640
Void ratio (%)	-	-	-	-	45.0
Water Absorption (%)	-	-	-	1.02	0.89

Table 4. Chemical composition of sodium hydroxide.

Chemical Composition	Array	Carbonate (CO_3)	Chloride (Cl)	Sulphate (SO_4)	Potassium (K)	Silicate (SiO_2)	Zinc	Size
Percentage	98	1.6	0.01	0.04	0.2	0.05	0.02	3–7mm

Table 5. Chemical composition of sodium silicate.

Chemical Composition	Na_2O (%)	SiO_2 (%)	Ratio of Na_2O to SiO_2	Total solid (%)	Water content (%)
Percentage	16.65	34.35	1:2.06	51.00	49.00

Mix Proportions and Mechanical Properties

The composition of M35 grade concrete for this study was adapted from previous research [11, 22] in alignment with IS 10262 standards. The proportions of binder, fine aggregate, coarse aggregate, and liquid were established as 390 kg/m^3, 695 kg/m^3, 1115 kg/m^3, and 200 kg/m^3, respectively. To achieve M35-grade GPC, different mix ratios of FA and GGBS were investigated, including ratios of 100:0, 80:20, 60:40, 40:60, 20:80, and 0:100, and all these mixes were compared with conventional concrete with complete cement. The mix identification names were selected as S0 to S6, where S0 represents 100% cement, and S1 represents 100% FA and 0% GGBS. The liquid-to-binder ratio was adjusted within the range of 0.45 to 0.53 to ensure optimal consistency. The alkaline liquid for all the mixes at 2.5. In geopolymer concrete formulations, river sand was entirely substituted with M-Sand. GPC samples were produced using class F-FA sourced from Qcrete Ready-Mix (India) Pvt. Ltd., located in Bettahalasuru Indian Village, Bangalore. Commercial GGBS was used as a partial replacement for FA. The Alkali Activated Solution (AAS) was developed by combining sodium silicate and sodium hydroxide. Before use, 8M NaOH solution prepared before 24 hr. This mixture was then blended with Na_2SiO_3 solution to form an alkaline activator solution, enhancing solution reactivity. During the mixing process, the aggregates were initially combined in a mixer under Saturated Surface Dry conditions. Subsequently, the binder components were introduced into the aggregate mixture and mixed for approximately 3 minutes. Pre-prepared AAS was then added to the mixer, and blending continued for about 4 minutes, ensuring uniformity and achieving the desired consistency of the concrete. The mechanical properties of the GPC and conventional concretes are summarized in Table 6.

Methods

The geometric parameters of wall facing elements, including area, volume, perimeter, and centroid, are vital in optimizing their interlocking performance. A thorough understanding of these parameter's aids in the preparation of components that contribute to stable and durable masonry structures. By integrating this knowledge, improved wall facing interlock systems can be developed, enhancing the overall efficiency and reliability of construction projects. The dimensions of the wall facing interlock system shown in Figure 1 and Table 6.

Beam Details and Preparation

For each mixture, three concrete beams were created with dimensions 150 mm in width, 150 mm in depth, and 700 mm in length. After preparing the geopolymer concrete mixture, it was promptly poured into the beams. Simultaneously, piezoelectric sensors were positioned at varying depths within the beam. These sensors are commonly used and cost-effective tools for crack detection in concrete, showing signal changes under mechanical stress. A group of 5 sensors were strategically placed at different depths and spacings 37.5 cm as shown in Figure 2. The concrete mixture was poured in three layers and compacted in beam Molds. After 24 hours, the specimens were demolded and subjected to ambient curing for GPC and water curing for conventional concrete, both for a duration of 28 days.

Figure 1. Wall facing interlock.

Table 6. Detail of interlock.

Parameter	Value
Area	497 cm^2
Volume	2485 cm^3
Perimeter	100
Centroid	X direction-2131.6 mm Y direction-2110.7 mm

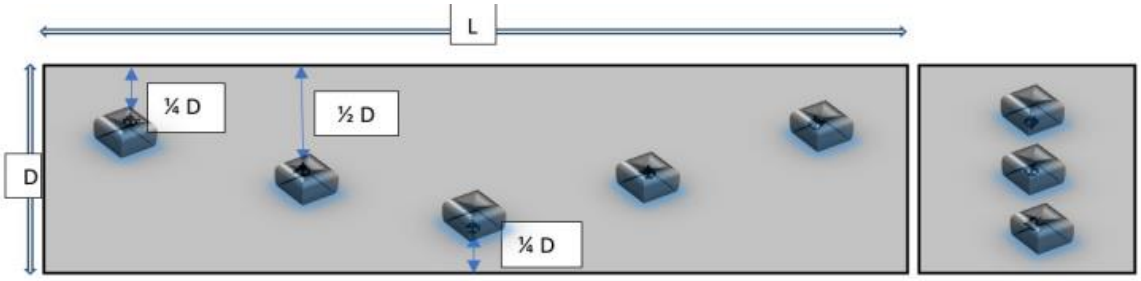

Figure 2. Wall Facing Interlock (Xiaolong Liao et al., 2023).

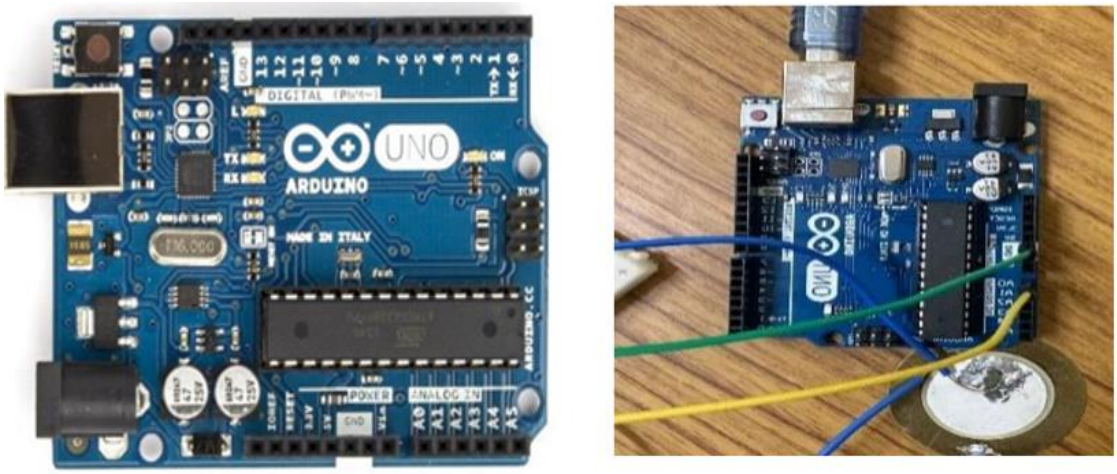

Figure 3. (a) Arduino Uno Board and (b) Breadboard.

Arduino Uno

Arduino Uno is a microcontroller board with 14 digital I/O pins, 6 analog inputs, USB connectivity, and a 16 MHz resonator as shown in Figure 3 (a). It lacks the FTDI chip, using Atmega16U2 (or Atmega8U2) as a USB-to-serial converter. Connect to a computer or power source to start programming and experimentation.

Breadboard

Breadboard is a part of the circuit system used to create the circuit without doing any complex design and soldering available in different sizes and temporary connections are made using breadboard as shown in Figure 3 (a) and (b). These boards have many tiny sockets (holes) components of the circuit are inserted in these tiny holes; single core plastic coated wires are used for the connections.

Resistors

Resistors are passive components with two terminals that impede electrical current flow. They regulate current, signal levels, isolate voltages, and more in electronic circuits. Fixed resistors maintain resistance despite temperature or voltage changes. Variable resistors adjust circuit elements like volume controls or sensors for heat, light, humidity, force, or chemical activity. PZT Sensors, is

capable of detecting and measuring vibrations in the concrete structure. This is crucial for identifying any anomalies or changes in structural behavior that may indicate damage or deterioration. The sensor can be used to assess the elastic properties of concrete in situ. This includes measuring parameters such as Young's modulus, Poisson's ratio, and other material properties that are indicative of the structural integrity of the concrete. The majority of PEHs are made from crystalline materials, such as piezo ceramics or piezoelectric polymers. Lead-zirconate-titanate has a high cost-effectiveness because of its high-cost effectiveness (PZT) as shown in Figure 4 it is used in various applications. by turning variations in force, strain, temperature, acceleration, or pressure into an electrical charge. They are measured using the piezoelectric sensor effect.

EXPERIMENTAL METHODS

The selection of 20 mm diameter and 1 mm thick circular PZT patches was a pivotal aspect of this study, with meticulous consideration. To ensure proper alignment, the PZT patches underwent polarization in the direction of their thickness, as depicted in Figure 5. Importantly, the deliberate orientation of the PZT material in the 3-direction aligned it with the out-of-plane direction of the patch. Lead wires were securely attached to the terminals at opposite ends of the PZT patches. The choice of PZT patches was based on their ability to maintain d33 values with minimal change within the range of 2-3%. To shield the PZT patches from potential damage due to moisture and the alkaline qualities of the surrounding concrete environment, a dual-layer protective approach was implemented, involving the combination of epoxy and hydrophobic coating.

The thickness of the epoxy layer surrounding the PZT patch served two objectives: effective insulation from the surrounding concrete medium and heightened sensitivity to variations inside the concrete structure. In the empirical phase of the investigation, transient vibration data were collected using implanted PZT sensors within conventional concrete beams measuring 150 mm x 150 mm x 700 mm. These sensors played a crucial role in capturing the dynamic vibrational motion resulting from external input. Vibration measurements were conducted at designated time intervals, around 12 hours post-casting and subsequent removal from molds. Five PZT sensors were strategically placed within the concrete, parallel to the top surface of the mold, with one sensor positioned horizontally. These sensor positions were deliberately chosen to be at a distance from nodal points of the beam's primary vibration modes and a safe distance from the beam's edges. The collected transient vibration patterns provided insights into the developmental progress of the elastic characteristics in the hydrating concrete under specific conditions. The vibrational measurements utilized embedded PZT sensors and accelerometers securely attached to the concrete beam. Following this, the beams underwent loading using a flexural strength testing apparatus. Arduino Uno facilitated the establishment of a linkage between the accelerometer and two embedded PZT sensors. Signals from these sensors were captured at a sample frequency of 100 kHz, resulting in datasets containing 10,000 individual data points per dataset, as depicted in Figure 6.

Figure 4. Piezoelectric sensors.

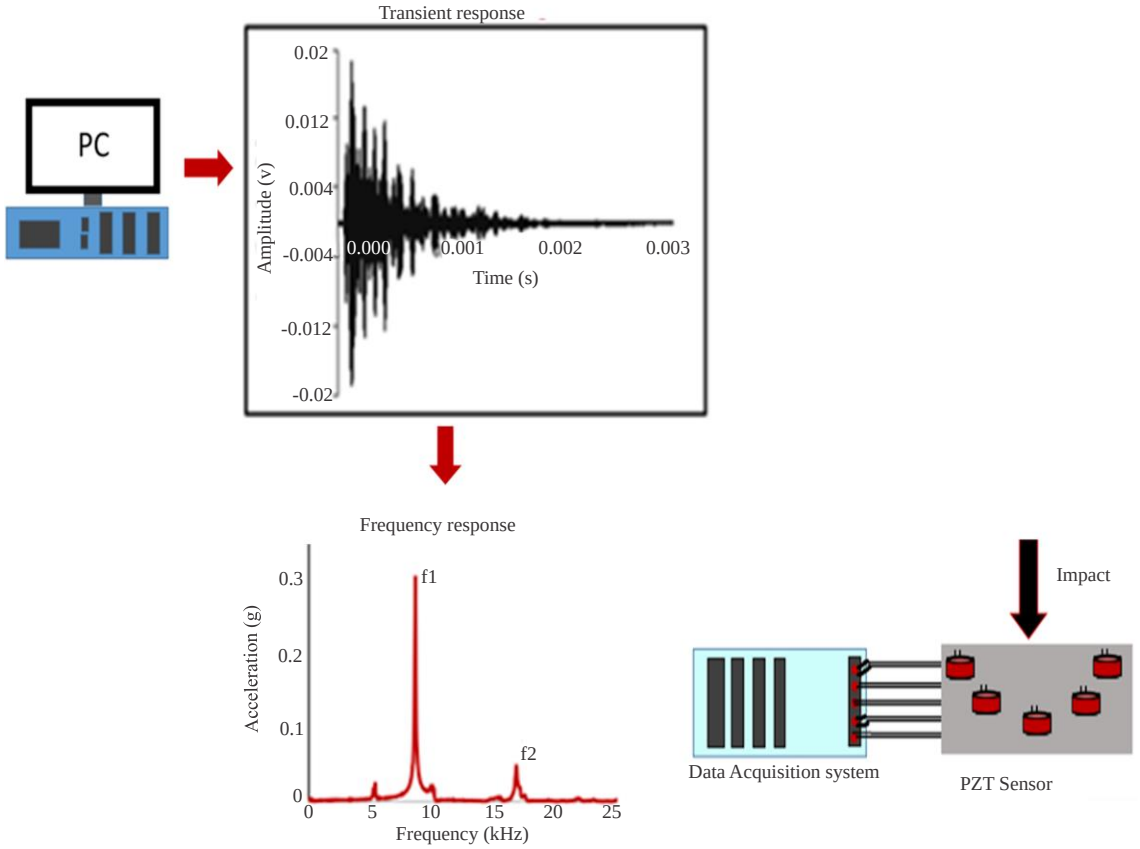

Figure 5. Schematic Representation of the experimental test setup for vibration measurement (Xiaolong Liao et al., 2023).

Figure 6. Testing of specimen.

The vibration data collection occurred after a curing period of 28 days, documenting the vibrational characteristics. The flexural strength test, as shown in Figure 7, adhered to IS Code Book guidelines, employing a flexural testing apparatus. The specimen was positioned on supports, ensuring equal spacing on both sides, with its longitudinal axis perpendicular to the applied load. Incremental load application allowed the calculation of the specimen's strength. Software applications were employed to determine unknown proportions of Ground Granulated Blast Furnace Slag (GGBS) and Fly Ash by inputting and outputting the acquired strength values.

EXPERIMENTAL RESULTS

Compressive Strength of Geopolymer Concrete

Compressive strength stands as a vital property in assessing hardened concrete, serving as its characteristic material value for classification. This study followed BS EN 12390-3:2002 guidelines, conducting compressive strength tests with a 2000 KN Digital Compressive & Flexural Testing Machine in the Concrete Laboratory. Each mix underwent testing with a set of three cubes after a 1-day curing period. The average compressive strength for each mix composition is detailed in Table 7. Compressive strength is a fundamental measure of concrete's durability and longevity. During the study, specimens with 100% FA content had to be extracted from molds after 20 hours since they didn't achieve the necessary hardening within one day. The compressive strength of nominal mix is 42.65 N/mm^2. The low CaO content in FA affects GPC's initial setting time. Yet, the introduction of GGBFS into FA-based geopolymer concrete expedited setting. Notably, Figure 8 illustrates the substantial enhancement in the compressive strength of SCGC due to GGBFS inclusion. The highest result was found in the ratio of 40% Flyash and 60% GGBS after that there is slight reduction in strength due to excessive amount of alkaline liquid and calcium. The sufficient bonding is happened the mix of S4.

Figure 7. Setup for testing specimen with sensors.

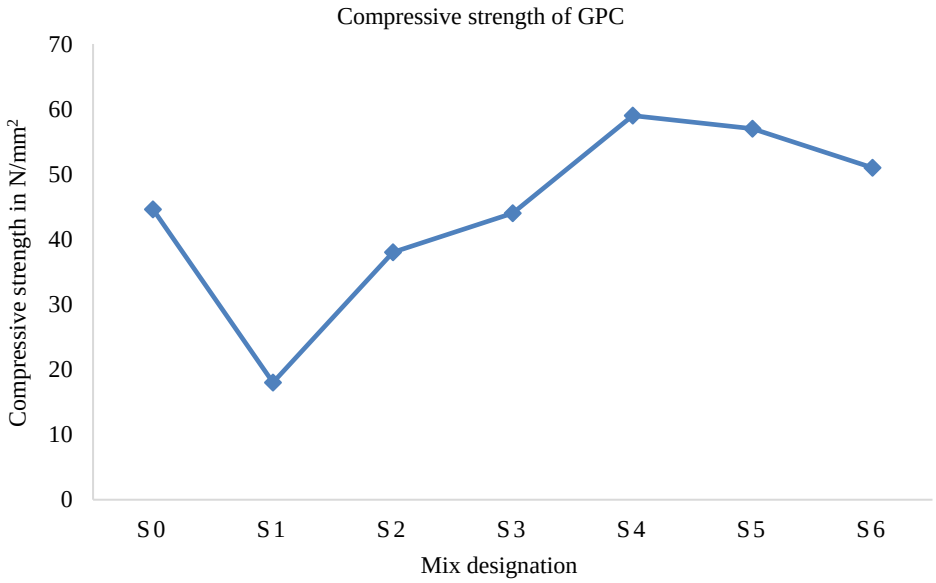

Figure 8. Effect of fly ash & GGBS level on compressive strength.

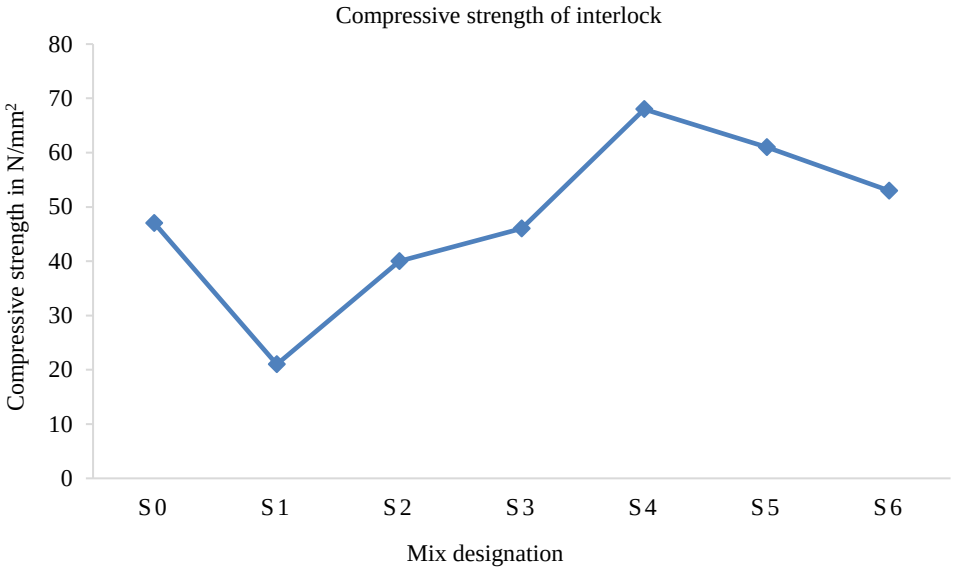

Figure 9. Compressive strength of interlocks.

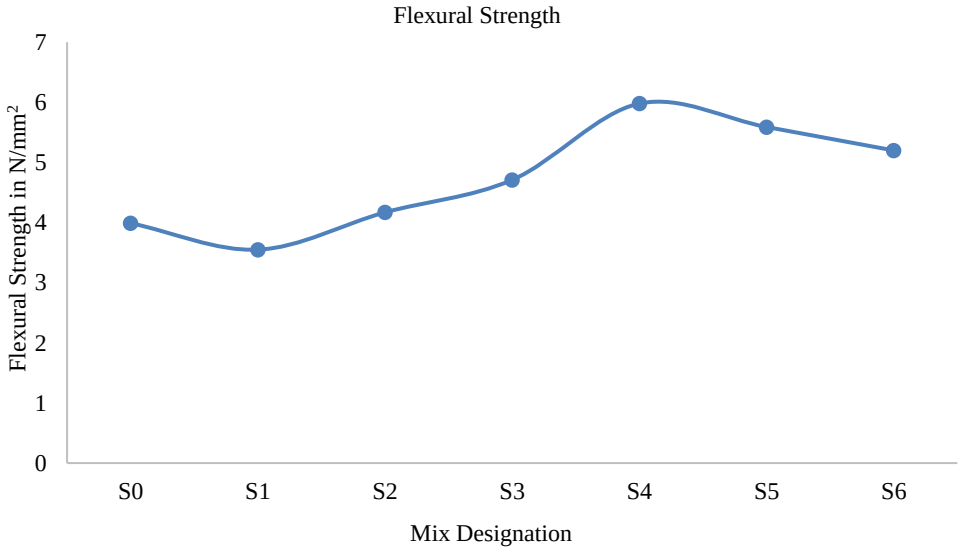

Figure 10. Effect of fly ash & GGBS level on flexural strength.

Geopolymers' compressive strength is influenced by factors such as the chemical composition, alkaline activator concentration, curing conditions, water-to-binder ratio, particle size, and the quality of raw materials.

Compressive Strength of Interlocks

The compressive strength of interlocks created with geopolymer concrete closely resembles that of GPC cubes. In fact, the strength of the interlocks can exceed that of cubes by 5 to 12%. This enhancement can be attributed to the difference in surface area. While a cube has an area of 100 mm per side, the interlock boasts an area of 497 cm². Consequently, this interlock variation holds promise for utilization in highway construction and is worth considering as shown in Figure 9.

Flexural Strength of Geopolymer Concrete

The graph depicts the average flexural strength values of three specimens for various curing periods. From the Figure 10, it is evident that after a 28-day air curing period, the flexural strength is

3.99 N/mm^2 for 100% cement, 5.2 N/mm^2 for 100% GGBS, and 3.55 N/mm^2 for 100% Fly ash. As a result, it can be concluded that the highest strength is achieved for specimens composed of 40% Fly ash and 60% GGBS, measuring 5.98 N/mm^2. Moreover, it is noticeable that the strength declines as the percentage of Fly ash increases.

Durability Test

Determination of durability outcomes involved subjecting 100 mm × 100 mm × 100 mm cubes to hydrochloric acid solution, prepared by blending 5% HCl with 1000 ml water as shown in Figure 11. The weight measurements of the cubes were taken at distinct intervals 7, 14, and 28 days. Notably, the combination of 60% GGBS and 40% fly ash exhibited minimal weight reduction, surpassing all other ratios. Additionally, this same ratio demonstrated comparatively lower diminution in compressive strength. Consequently, it is deduced that the composition with 60% GGBS and 40% fly ash offers superior durability against acid-induced deterioration. The test results are showed in Table 7 and 8 respectively.

Figure 11. Blocks immersed in solution.

Table 7. Weight of sample for different age in days.

Samples	Initial weight	7 days (kg)	14 days (kg)	28 days (kg)	Percentage wt. decrease at 28 days (%)
S0	2.426	2.370	2.341	2.305	4.99
S1	2.535	2.520	2.513	2.496	1.54
S2	2.504	2.488	2.469	2.459	1.80
S3	2.609	2.598	2.590	2.581	1.07
S4	2.539	2.523	2.513	2.494	1.77
S5	2.497	2.488	2.472	2.458	1.94
S6	2.505	2.492	2.484	2.436	2.44

Table 8. Compressive strength (N/mm^2) test of cubes after curing in HCl solution.

Samples	28 days strength in N/mm^2 Before the test	28 days strength after Durability test in N/mm^2	Percentage (%) decrease in strength
S0	42.65	32.63	23.49
S1	21.23	11.43	46.16
S2	38.65	34.55	10.61
S3	46.86	41.90	10.58
S4	63.79	61.65	3.35
S5	58.23	54.33	6.70
S6	52.22	46.56	6.51

To evoke the longitudinal vibration modes inherent in the concrete beam, impact was precisely administered at the center of one of its surfaces. In parallel, an accelerometer was affixed to the center of the opposing surface, enabling the capture of the ensuing transient response. Simultaneously, transient responses were also registered from the integrated PZT sensors. The acceleration data recorded by the accelerometer during a typical impact event was graphically put together with the voltage outputs derived from the PZT sensors as shown in Table 9. Evidently, the dynamic transient motion of the beam, propagated through waves, was distinctly discernible within the voltage responses of the PZT sensors. In order to further analyze the responses, the transient data in the time-domain underwent a frequency-domain transformation. Peaks observed in the frequency domain representation of the transient acceleration response, as captured by the accelerometer, corresponded to the longitudinal resonance modes intrinsic to the beam's behavior. Crucially, all PZT sensors demonstrated the capacity to effectively capture these longitudinal resonance modes within the concrete beam. The longitudinal motion of the structure induced an expansion and contraction phenomenon within the medium's plane. This motion was aptly captured by the PZTs, oriented with polling directions both perpendicular and parallel to the direction of stress wave propagation. In the graphical representation, the x-axis denoted Frequency (kHz), while the y-axis represented Acceleration (g).

Specifically, Figures 12, 13, and 14 displayed the frequency characteristics of different mix compositions with varying proportions of GGBS and Flyash within the geopolymer concrete. This comprehensive data set was also tabulated in Table 9, encompassing frequency values in kHZ for all the distinct mix variations. Notably, the maximum frequency was achieved in the mix comprising 60% GGBS and 40% Flyash, indicating heightened resistance to impact loads compared to other mix compositions. Subsequently, an observable reduction in frequency was noted as the flyash content increased within the mixtures.

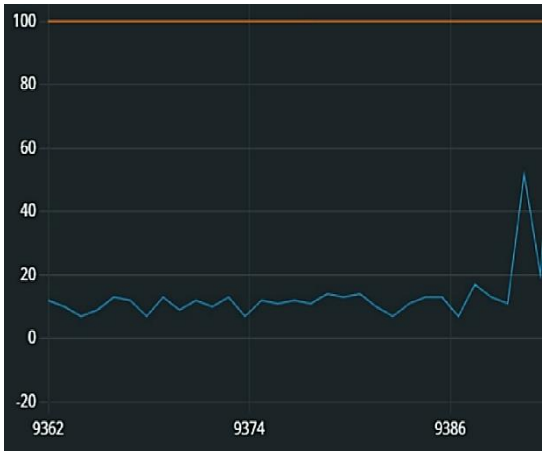

Figure 12. The conductance and susceptance of the embedded PZT sensor measured for 40% GGBS and 60% flyash.

Figure 13. The conductance and susceptance of the embedded PZT sensor measured for 100% GGBS and 0% flyash.

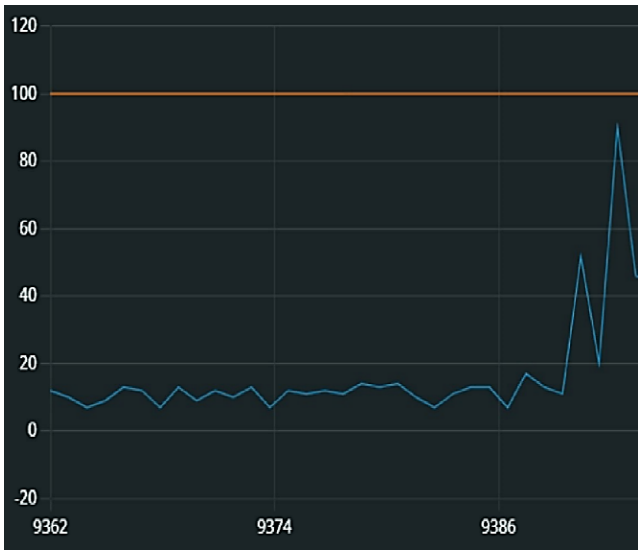

Figure 14. The conductance and susceptance of the embedded PZT sensor measured for 60% GGBS and 40% flyash.

Table 9. Maximum vibrations for different mix proportions.

Mix Proportion	Maximum Vibrations	Failure Load
S0	60	22
S1	80	25
S2	88	30
S3	65	20
S4	50	18
S5	45	10

CONCLUSIONS

A novel PZT-based sensor suitable for embedding within concrete structures is designed through a multi-layer protection approach. This design strategy ensures the sensor's safeguarding against physical damage, moisture ingress, and exposure to chemical agents. The resultant PZT sensor exhibits exceptional sensitivity in capturing the transient vibrational behavior of concrete structures post-setting. In summary, the specific implications drawn from the research findings presented in the paper are:

- The study delved into several significant aspects of geopolymer concrete, revealing key findings that contribute to the advancement of concrete technology. The investigation of compressive strength showcased the intricate interplay of materials, emphasizing the impact of varying proportions of fly ash (FA) and ground granulated blast furnace slag (GGBFS) on strength and hardening properties. Notably, the inclusion of GGBFS expedited setting times, leading to enhanced compressive strength. The most substantial gains were observed in the mix with 40% fly ash and 60% GGBFS, demonstrating superior bonding and strength.
- Moreover, the research extended to assess flexural strength, uncovering the strengths of distinct compositions over different curing periods. The results underscored the significance of balanced proportions, with 40% fly ash and 60% GGBFS emerging as the optimal composition, offering elevated flexural strength and resilience.
- The investigation's focus on durability yielded insights into acid resistance, a critical factor in concrete longevity. The durability assessment showcased that the mix of 60% GGBFS and 40% fly ash exhibited remarkable resistance to acid-induced deterioration, an attribute attributed to its distinctive composition. This finding provides valuable guidance for applications requiring resistance to corrosive environments.
- The exploration of vibration responses introduced the innovative application of PZT sensors, highlighting their effectiveness in capturing dynamic structural behaviour. These sensors proved capable of recording longitudinal resonance modes within concrete beams, offering valuable insights into material behaviour under stress. The data obtained through this analysis, along with the frequency characteristics of various mix compositions, contributes to the understanding of concrete behaviour and its potential implications in structural design.

Acknowledgments

Extending sincere gratitude esteemed co-authors, Dr. Chandrashekar A and Dr. Ananthayya M B, for their invaluable contributions to this journal. Our heartfelt appreciation also goes to the management of Nitte Meenakshi Institute of Technology and KVG College of Engineering for their unwavering support, which played a crucial role in the successful completion of the research work. We are grateful for their instrumental assistance and gracious provision of access to all necessary facilities.

REFERENCES

1. Constantin, E.C.; Chris, G.K.; Georgia, M.A.; et al., *Application of smart piezoelectric materials in a wireless admittance monitoring system. (WiAMS) to structure - Test in RC elements.* Case Stud. Constr. Mater. 2016, 5, 1–18.
2. Priya, B.; Thiyagarajan, J.; Monica, B.; et al., *EMI based monitoring of early-age characteristics of concrete and comparison of serial/parallel multi-sensing technique*. Constr. Build. Mater. 2018, 191, 1268–1284.
3. Bakharev T, *Resistance of Geopolymer Materials to Acid Attack*, Cement and Concrete Research, 35, 2005, 658–670, https://doi.org/10.1016/j.cemconres.2004.06.005
4. Raijiwala D B and Patil H S, *Geopolymer concrete, a green concrete*, Institute of Electrical and Electronics Engineers, 2nd Int. Conf. on Chemical, Biological and Environmental Engineering 2010 (Cairo, Egypt, Nov.)
5. Y H M Amran, R Alyousef, H Alabduljabbar M et al., *Clean production and properties of geopolymer concrete; a review*, J. Clean. Prod. 251 2020, 119679.
6. Hussein Hamada, Bassam Tayeh, Fadzil Yahaya, et al., *Effects of nano-palm oil fuel ash and nano-eggshell powder on concrete*, Construction and Building Materials, 2020, Volume 261, 119790, ISSN 0950-0618, https://doi.org/10.1016/j.conbuildmat.2020.119790.
7. Tayeh B.A., H. Hanoona, M. Alqedra, et al., *Investigating the effect of sulfate attack on compressive strength of recycled aggregate concrete*, J. Eng. Res. Technol. 4 (4) (2017).
8. Amin M., B.A. Tayeh, *Investigating the mechanical and microstructure properties of fibre-reinforced lightweight concrete under elevated temperatures*, Case Stud. Constr. Mater. 13, 2020, e00459.

9. Hussein M Hamada, Blessen Skariah Thomas, Bassam Tayeh, et al., Use of oil palm shell as an aggregate in cement concrete: A review, Construction and Building Materials, 2020, Volume 265, 120357, ISSN 0950-0618, https://doi.org/10.1016/j.conbuildmat.2020.120357.
10. Tayeh B.A., M.W. Hasaniyah, A.M. Zeyad, et al., *Durability and mechanical properties of seashell partially- replaced cement*, J. Build. Eng. 31 (2020), 101328.
11. Moulya H.V, Vikram Kedambadi Vasu, Praveena B.A, et al., *Study on acoustic properties of polyester – Fly ash Cenosphere\Nanographene composites*, Materials Today: Proceedings, 2022, Volume 52, Part 3, Pages 1272–1277, ISSN 2214-7853, https://doi.org/10.1016/j.matpr. 2021.11.052.
12. Hassan A M. Arif, M. Shariq, *A review of properties and behaviour of reinforced geopolymer concrete structural elements- a clean technology option for sustainable development*, J. Clean. Prod. 245 (2020), 118762.
13. Tayeh B A, D M Al Saffar, A S Aadi, et al., *Sulphate resistance of cement mortar contains glass powder*, J. King Saud Univ.-Eng. Sci. (2019).
14. Alaloul W S, M A Musarat, B A Tayeh, et al., *Mechanical and deformation properties of rubberized engineered cementitious composite (ECC)*, Case Stud. Constr. Mater. 13 (2020), e00385.
15. Laflamme S, SaleemH, VasanB, et al., *Elastomeric capacitor network for strain sensing over large surfaces.* IEEE/ ASME Trans Mech 2013; 18:1647–54.
16. Laflamme S, Kollosche M, Connor JJ, et al., *Robust flexible capacitive surface sensor for structural health monitoring applications.* ASCE J EngMech 2012; 139:879–85.
17. Wen S, Chung D, *Model of piezo resistivity in carbon fiber cement.* Cem ConcrRes2006; 36:1879–85.
18. J Pan, C Zhang, X Zhang, et al., *Real-time accurate do meter velocity estimation aided by accelerometers*, Measurement 91(2016)468–473.
19. S.Kavitha, R.J.Daniel, K.Sumangala, *Design and analysis of MEMS comb drive capacitive accelerometer for SHM and seismic applications*, Measurement 93 (2016) 327–339.
20. A.Venugopal, A.Agrawal, S.V.Prabhu, *Performancee valuation of piezoelectric and differential pressure sensor for vortex flowmeters*, Measurement 50(2014) 10–18.
21. Y J Li, G C Wang, J.Zhang, Z.-Y.Jia, *Dynamic characteristics of piezoelectric six dimensional heavy force/moment sensor for large-load robotic manipulator*, Measurement 45(2012)1114–1125.
22. H.V. Moulya, A. Chandrashekhar, *Experimental Investigation of Effect of Recycled Coarse Aggregate Properties on the Mechanical and Durability Characteristics of Geopolymer Concrete*, Materials Today: Proceedings, 2022, Volume 59, Part 3, Pages 1700–1707, ISSN 2214-7853, https://doi.org/10.1016/j.matpr.2022.03.403.
23. A Maekawa, T Takahashi, T Tsuji, et al., *Experimental validation of non-contacting measurement method using LED-optical displacement sensors for vibration stress of small-borepiping*, Measurement 71(2015)1–10.
24. J G Chen, N Wadhwa, Y J Cha, *Modal identification of simple structures with high-speed video using motion magnification*, J.Sound Vib.345(2015)58–71.
25. D Lau, Q Qiu, *Are view of non-destructive testing approached using mechanical and electromagnetic waves*, Proceedings of the SPIE 9804, Non-destructive Characterization and Monitoring of Advanced Materials, Aerospace, and Civil Infrastructure 2016, 98042E, April22,2016, Las Vegas, Nevada, United States, (2016).
26. C Hsiao, C C Cheng, T Liou, et al., *Detecting flaws in concrete blocks using the impact-echo method*, NDTandEInt.41(2008)98–107.
27. Xiaolong Liao, Qixiang Yan, Haojia Zhong, et al., *Integrating PZT-enabled active sensing with deep learning techniques for automatic monitoring and assessment of early-age concrete strength.* Volume 211, April 2023, 112657 https://doi.org/10.1016/j.measurement.2023.112657

